Jour. Geol. Soc. Japan, Vol. 105, No. 9, p. 625–642, September 1999

Coeval volcanism due to interaction of back-arc basin basalt (BABB) magma with the island-arc crust in the late Miocene Engaru volcanic field, northeastern Hokkaido, Japan : The evidence of Sr and Nd isotopic ratios combined with major- and trace-element compositions

*Satoshi Yamashita**, *Kenji Shuto***, *Yasuyuki Kakihara**** *and Hiroo Kagami****

Received July 23, 1998.
Accepted April 20, 1999.

* Fukken Gijutu Consultants Co.Ltd., Nishiki-cho 1-7-25, Aoba-ku, Sendai 980-0012, Japan
** Department of Geology, Faculty of Science, Niigata University, Ikarashi 2-machi 8050, Niigata 950-2181, Japan
*** Graduate School of Science and Technology, Niigata University, Ikarashi 2-machi 8050, Niigata 950-2181, Japan

Abstract

The late Miocene Engaru volcanic field in northeastern Hokkaido contains basalts, Tomeoka basalt (TM) and Chiyoda-Kakurezawa basalt (CK), and rhyolite, Wakamatsu rhyolite (WK), with subordinate amounts of andesite, Sakaeno andesite (SK), which erupted during 7–9 Ma.

Both the TM and CK basalts have geochemical characteristics similar to those of back-arc basin basalt (BABB). Based on differences in major and trace element abundances and the initial values of Sr and Nd isotopic ratios (SrI and NdI), the CK basalt, SK andesite and WK rhyolite can be divided into two types (I and II), respectively. The SK type I andesite and WK type I rhyolite are of calc-alkaline series, whereas the SK type II andesite (including icelandite-like andesite) and WK type II rhyolite are of tholeiitic series.

The WK type I rhyolite has remarkably high SrI and low NdI values compared with other volcanic rocks from the study area. The similarity in SrI of the rhyolite to S-type granitoids and pelitic-psammitic rocks of the Hidaka belt suggests the crustal origin of the rhyolite. The combined major- and trace-element and Sr- and Nd- isotopic data indicate that the main generation process of the SK type I andesite was the mixing of basaltic magma (the CK type I basalt) with some felsic magmas. The felsic magmas are the WK type I rhyolite magma and rhyolitic magmas having higher Sr and Nd contents, and higher SrI and lower NdI values than the WK type I rhyolite. On the other hand, the SK type II andesite and WK type II rhyolite may have been derived from the CK type II basaltic magma by fractional crystallization accompanied by a minor degree of assimilation of crustal materials.

The genetic relationship of these coeval basalts, andesite and rhyolite can be attributed to spreading of the Kurile basin. BABB magma which is a partial melt in a hot asthenosphere uprising below the island arc during the basin spreading, could have heated the crust to generate calc-alkaline rhyolitic magma. Andesitic rocks were derived both by mixing of BABB magma with the crust-derived rhyolitic magma and by fractional ctystallization of BABB magma.

Key words : Engaru district, North Hokkaido, Late Miocene, back-arc basin basalt, crust, magma mixing, fractional crystallization, Sr and Nd isotopes, spreading of the Kurile basin

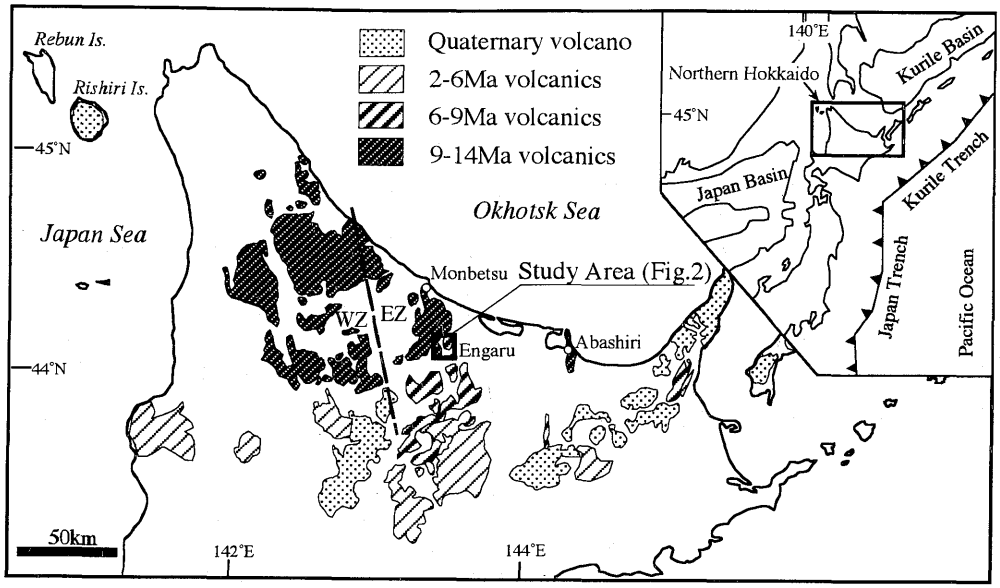

Fig. 1. Index map showing the study area and distribution of Cenozoic volcanic rocks in northern Hokkaido, Japan. Boundary of western (WZ) and eastern (EZ) zones is slightly modified from Watanabe and Yamaguchi (1988).

Introduction

Tertiary volcanic rocks in north Hokkaido are widely distributed in a back arc region behind the junction of the Northeast Japan and Kurile arcs (Fig. 1). K-Ar age data for these volcanic rocks indicate that an intense volcanic activity has taken place since about 14 Ma (e.g., Shibata et al., 1981 ; Watanabe et al., 1991 ; Nakagawa et al., 1993 ; Goto et al., 1995 ; Sugawara et al., 1995 ; Yahata and Nishido, 1995 ; Aoki et al., 1999). Recent works have revealed regional petrological and geochemical differences in middle to late Miocene (6-14 Ma) volcanic rocks between the eastern and western regions (Kokubu et al., 1994 ; Watanabe and Yamaguchi, 1988 ; Goto et al., 1995 ; Okamura et al., 1995). Rocks in the eastern region (northeastern Hokkaido) are characterized by non-island arc type volcanics, including icelandite-like andesite, basalt and andesite enriched in TiO_2, and voluminous calc-alkaline dacite and rhyolite. Rocks in the western region (northwestern Hokkaido) are characterized by large amounts of calc-alkaline andesites.

Based mainly on petrologic and geochemical data, the following models have been proposed as the tectonic background for the generation of these volcanic rocks ; a volcanic activity was caused by back-arc spreading related to the formation of the Kurile basin (Goto et al., 1995 ; Ikeda, 1998), due to an increase in the dip-angle of the subducting Pacific plate and resulting injection of hot asthenosphere (Watanabe, 1995), or due to during collision of the Eurasian, Okhotsk and Pacific plates (Okamura et al., 1995).

The Engaru district is located in northeastern Hokkaido, about 15 km inland from the Okhotsk Sea coast (Fig. 1), where an intense terrestrial volcanism associated with regional uplift took place during the middle to late Miocene. Recent K-Ar age determinations show that volcanic rocks were erupted during two periods of volcanic activity (Yahata and Nishido, 1995). The first episode (11-13 Ma) involves eruption of andesitic magma, whereas the second episode (7-9 Ma) involves eruption of voluminous basalt and rhyolite magmas accompanied by small amounts of andesite magma.

In this paper we examine the origin of coeval basalt, andesite and rhyolite produced during the second volcanic episode, and show that this activity was caused by the interaction of BABB magma with island arc crust, resulting from upwelling of asthenospheric mantle during spreading of the Kurile basin.

Stratigraphy

Tertiary volcanic rocks are exposed over a 15 km (N-S) × 12 km (E-W) area in the Engaru district, northwestern Hokkaido (Fig. 2). Lithologically volcanic rocks can be divided into six units ; in the ascending order, the Inaushi andesite (IN andesite), Gakenosawa tuff (GK tuff), TM basalt, WK rhyolite, SK andesite and CK basalt (Fig. 3). The SK andesite interfingers with the WK rhyolite. The IN andesite and GK tuff were possibly erupted in the middle Miocene (11-13 Ma), while the TM basalt, WK rhyolite, SK andesite and CK basalt were emplaced during the late Miocene (7-9 Ma).

1. Inaushi andesite

The IN andesite is restricted to the south of the district (Fig. 2), and is composed of massive lava flows and pyroclastic rocks (tuff breccia and volcanic breccia) with a total thickness of about 500 m. They are underlain and overlain by sedimentary rocks. The underlying sedimentary rocks consisit mainly of sandstone with intercalations of conglomerate and mudstone (50 to 70 m thick), and unconformably over-

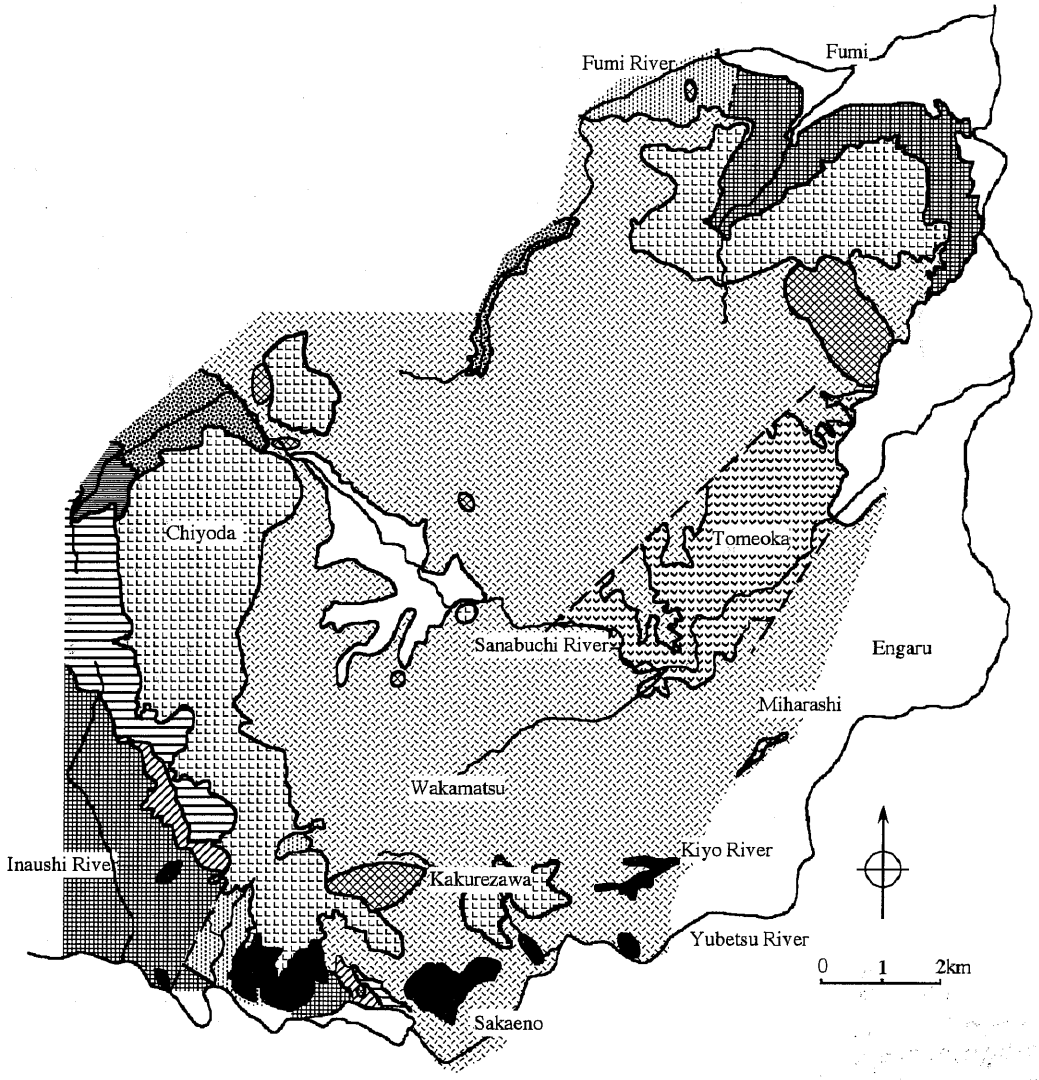

Fig. 2. Geologic map of the Engaru district. See Fig. 1 for location.

lie the late Cretaceous Hidaka Formation.

To the west of this area is extensive exposures of andesite (the Kohonomai Formation), which corresponds both stratigraphically and lithologically to the IN andesite. Two specimens from the Kohonomai Formation have K-Ar ages of 11.4 Ma and 12.8 Ma (Yahata and Nishido, 1995).

2. Gakenosawa tuff

The GK tuff is found as isolated exposures in the south and north of the district (Fig. 2). It is composed of beds of weakly altered, gray to white glassy tuff containing angular glassy clasts of about 1 cm in diameter. The thickness of the tuff beds is uncertain because of their poor exposure. Geological mapping

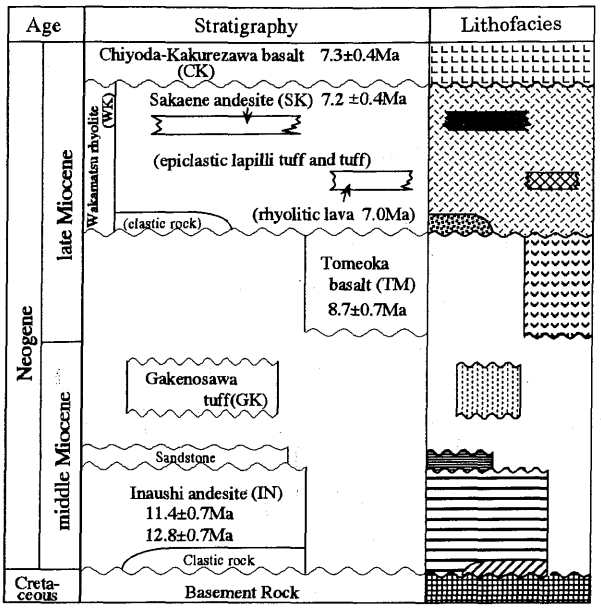

Fig. 3. Stratigraphic sequences in the study area. K-Ar age data ; Yahata and Nishido (1995).

indicates an unconformable relationship between the GK tuff and the underlying IN andesite, and the probable eruptive age of the tuff between 11-12 Ma and 9 Ma.

3. Tomeoka basalt

The TM basalt is distributed in the east of the district, as massive lava flows associated with autobrecciated facies, and well-stratified hyaloclastite. The latter consists mainly of fine-grained basaltic fragments (2-3 mm in diameter) embedded in a matrix of fine-grained volcanic glass. The unit is more than 200 m thick, and shows no direct contact with the underlying the GK tuff. A K-Ar age of Yahata and Nishido (1995) for the TM basalt is 8.7 Ma.

4. Wakamatsu rhyolite

The WK rhyolite, which is extensively distributed in this district (Fig. 2), is composed of three different rock facies including layers of clastic rocks, felsic epiclastic lapilli tuff and tuff, and rhyolitic masses. Clastic rocks are found at the base of the rhyolite flows, and consist of about 30 meters of alternating beds of well-rounded conglomerates and weakly cross-bedded sandstones. Felsic epiclastic rocks are the most abundant constituent of the WK rhyolite. Weakly stratified layers of lapilli tuff contain subangular to subrounded clasts of fibrous pumice, obsidian and rhyolite in a white-colored matrix of fine-grained, unconsolidated volcanic glass and crystals of biotite and quartz. Rhyolitic masses of mappably various sizes, possibly consisting of lava flows and lava domes, occur at several locations, being sandwitched by layers of the felsic epiclastics. The total thickness of the WK rhyolite ranges from 200 to 300 m.

Layers of felsic epiclastics unconformably overlie the TM basalt at Miharashi in the east of the district. The age of the WK rhyolite is probably about 7 Ma, judging from a K-Ar age of the overlying SK andesite.

5. Sakaeno andesite

The SK andesite occurs as lava flows and pyoclastic rocks in the south of the district (Fig. 2). The maximum thickness of lava flows reaches about 200 m. The contact between the SK andesite and the layers of felsic epiclastics of the WK rhyolite is observed north of a dam on the Yubetsu River at Sakaeno. The SK andesite may interfinger with the upper part of the WK rhyolite (felsic epiclastics).

Yahata and Nishido (1995) obtained a K-Ar age of 7.2 Ma for a sample from the Setaniushiyma andesite lava, which is a stratigraphically and lithologically correlative to the SK andesite.

6. Chiyoda-Kakurezawa basalt

Small-scale lava plateaus, consisting of basaltic lava flows and associated volcanic breccias, are distributed in topographically isolated, two high areas ; southwest of Chiyoda to Kakurezawa, and northeast of the study area. The CK basalt unconformably overlies the WK rhyolite (Fig. 3). These basaltic rocks are lithologically and petrographically similar to each other. The total thickness of the CK basalt is about 150 m.

A basalt specimen collected in a quarry at Kakurezawa yielded a K-Ar age of 7.3 Ma (Yahata and Nishido, 1995).

Petrography and mineral chemistry

The modal compositions of representative volcanic rocks from the five units, IN andesite, TM basalt, WK rhyolite, SK andesite and CK basalt are shown in Table 1.

1. Inaushi andesite

The IN andesite is porphyritic with between 16 and 34 vol% phenocrysts of plagioclase (9.6-29.0%), clinopyroxene (1.1-4.5%), orthopyroxene (0.8-5.2%) and Fe-Ti oxide (trace). Plagioclase phenocrysts are 1-3 mm long, and some grains have dusty zones. Fragmented and corroded plagioclase grains are also found. Clinopyroxene and orthopyroxene phenocrysts commonly form glomerporphyritic aggregates with plagioclase. The groundmass is hyalopilitic, and contains plagioclase microlites.

2. Tomeoka basalt

Phenocrysts in the TM basalt are hard to be identified from coarse grains in the groundmass. However, the TM basalt contains 2-6 vol% of euhedral and subhedral phenocrysts of olivine (2-5%) and plagioclase (less than 1%). Olivine phenocrysts (0.5-1 mm long) are generally fresh but are altered in part to clay minerals. Phenocryst plagioclase (0.5-2 mm long) is unzoned. The groundmass is intergranular, and consists of plagioclase, clinopyroxene, olivine,

Table 1. Modal compositions of volcanic rocks from the study area.

Sample No.	IN03	IN06	IN10	IN11	IN13	IN19	TM01	TM02	TM08	TM12
Phenocryst	16.2	32.4	24.8	22.1	20.7	33.6	2.7	2.3	2.9	5.5
Ol	-	-	-	-	-	-	2.7	2.3	2.9	4.8
Cpx	1.4	2.6	1.2	1.1	4.5	3.9	-	-	-	-
Opx	5.2	0.8	1.1	2.8	1.7	1.8	-	-	-	-
Bi	-	-	-	-	-	-	-	-	-	-
Fe-Ti oxide	-	-	r	r	r	-	-	-	-	-
Pl	9.6	29.0	22.5	18.2	14.5	27.9	-	-	r	0.7
Qz	-	-	-	-	-	-	-	-	-	-
Groundmass	83.8	67.6	75.2	77.9	79.3	66.4	97.3	97.7	97.1	94.5

Sample No. (type)	WK01 (type II)	WK06 (type I)	SK03 (type I)	SK06 (type I)	SK07 (type I)	SK10 (type II)	SK13 (type II)	SK17 (type II)	SK18 (type II)	CK04 (type II)	CK06 (type II)
Phenocryst	3.2	9.5	15.4	30.7	24.4	18.1	8.1	23.3	17.4	4.2	8.9
Ol	-	-	-	-	-	-	-	-	-	2.9	6.8
Cpx	-	-	0.4	2.8	2.9	1.3	2.4	2.8	2.6	-	-
Opx	-	-	4.5	3.9	2.6	0.5	r	0.1	0.7	-	-
Bi	-	1.1	-	-	-	-	-	-	-	-	-
Fe-Ti oxide	-	r	-	r	0.1	0.1	0.2	0.8	0.3	-	r
Pl	3.2	5.4	10.5	24.0	18.8	16.2	5.5	19.6	13.8	1.3	2.1
Qz	-	3.0	-	-	-	-	-	-	-	-	-
Groundmass	96.8	90.5	84.6	69.3	75.6	81.9	91.9	76.7	82.6	95.8	91.1

Sample No. (type)	CK12 (type II)	CK13 (type II)	CK15 (type II)	CK17 (type II)	CK23 (type II)	CK30 (type II)	CK31 (type II)	CK38 (type II)	CK48 (type I)	CK56 (type I)	CK60 (type I)
Phenocryst	1.0	22.8	11.6	23.4	24.0	5.8	11.0	7.1	5.5	6.8	4.0
Ol	0.6	5.8	8.3	7.1	5.7	-	2.4	2.1	2.9	2.8	2.0
Cpx	-	r	-	-	-	0.1	0.9	0.1	-	r	-
Opx	-	-	-	-	-	-	-	-	-	-	-
Bi	-	-	-	-	-	-	-	-	-	-	-
Fe-Ti oxide	-	r	-	-	-	-	r	-	-	-	-
Pl	0.4	17.0	3.3	16.3	18.3	5.7	7.7	4.9	2.6	4.0	2.0
Qz	-	-	-	-	-	-	-	-	-	-	-
Groundmass	99.0	77.2	88.4	76.6	76.0	94.2	89.0	92.9	94.5	93.2	96.0

Ol=olivine, Cpx=clinopyroxene, Opx=orthopyroxene, Bi=biotite, Pl=plagioclase, Qz=quartz, r=rare (modal %<0.1)
IN=Inaushi andesite, TM=Tomeoka basalt, WK=Wakamatsu rhyolite, SK=Sakaeno andesite,
CK=Chiyoda-Kakurezawa basalt

iron oxides and glassy mesostasis.

Cores of 10 to 20 grains of olivine phenocrysts for four samples show a relatively narrow compositional range (Fo%=74~85). Most olivine phenocrysts display slightly normal zoning.

3. Wakamatsu rhyolite

Based on the phenocryst mineral assemblage, rhyolitic rocks (constituting lava flows and lava domes) can be divided into two types. One type has 5-10 vol% phenocrysts of plagioclase (2-5%), corroded quartz (2-3%), biotite (~1%) and a minor Fe-Ti oxide, whereas the other type contains only plagioclase (about 3%) as a phenocryst phase. The groundmass of the former shows a heterogeneous feature in which a colorless glass is mingled with a brown glass containing plagioclase microlites, whereas the groundmass of the latter is hyalopilitic and less heterogeneous color.

4. Sakaeno andesite

The SK andesite is porphyritic, containing 8-31 vol % phenocrysts of plagioclase (6-24%), clinopyroxene (<1-3%), orthopyroxene (<1-5%) and Fe-Ti oxides (less than 1%). These minerals are found as not only discrete phenocrysts but also glomeroporphyritic aggregates of 2-3 mm in diameter.

The cores of orthopyroxene phenocrysts for six samples (SK 02, SK 03, SK 07, SK 13, SK 18 and SK 10) have a narrow Mg-value range (Fig. 4) showing a unimodal distribution, whereas those for two samples (SK 06 and SK 17) have a wide range showing a bimodal Mg-value distribution. Most orthopyroxene phenocrysts have uniform core compositions and are zoned normally in Mg in the margins (Fig. 5-A), but some phenocrysts are zoned reversely (Fig. 5-B).

Core compositions of clinopyroxene phenocrysts fall within ranges of Mg-value between 60 and 68 for SK 02, SK 18, SK 10 and SK 17, and between 68 and 74 for SK 13. Clinopyroxene cores in SK 06 also show a bimodal distribution (Fig. 4).

Although cores of plagioclase phenocrysts in seven andesite samples (except SK 06) have a relatively narrow compositional range in An% between 40 and

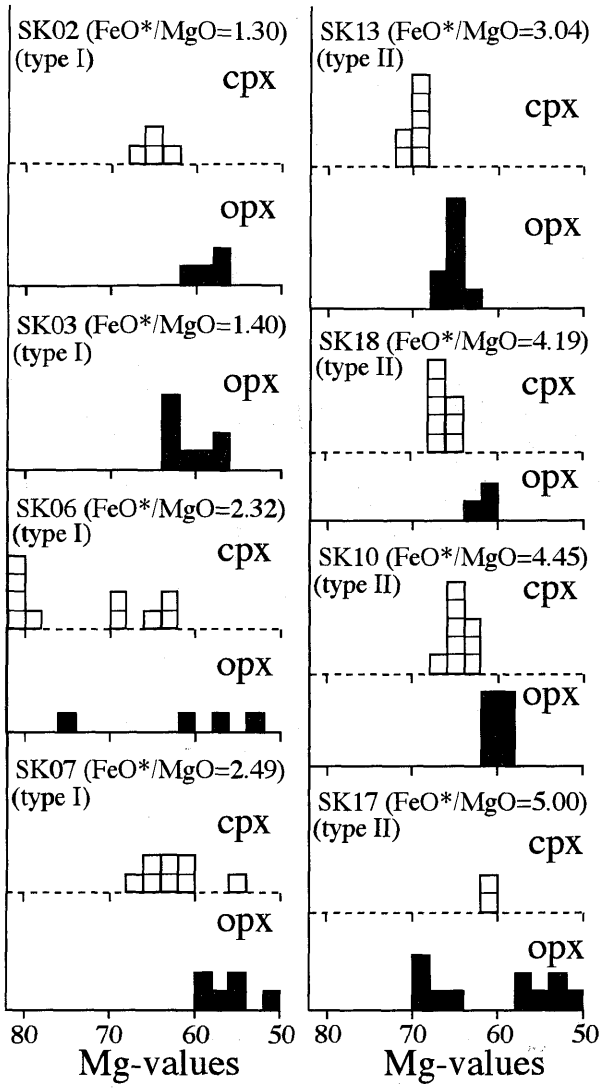

Fig. 4. Frequency of Mg values (Mg/(Mg+Fe)) of cores of clino- and ortho-pyroxene phenocrysts from the SK andesite. FeO*/MgO ratios are those of whole rocks.

56, those of SK 06 show a wide compositional range from An=40 to An=88. Although normal zoning is common among phenocryst plagioclases, reverse zoning is included in the latter plagioclases.

5. Chiyoda-Kakurezawa basalt

The CK basalt has 4 to 24 vol% phenocrysts, mostly less than 10%. Based on phenocryst assemblages, the basalt can be divided into two types ; one contains olivine (< 1 - 8%) and plagioclase (< 1 - 19%) phenocrysts, and the other contains olivine (2-3%), clinopyroxene (< 1%) and plagioclase (2 - 8%) phenocrysts. Fe-Ti oxide phenocrysts are rare in both types. One exceptional sample (CK 30) contains clinopyroxene, orthopyroxene and plagioclase phenocrysts but no olivine.

Olivine phenocrysts are up to 2 mm in length, and partly altered to clay minerals. Plagioclase phenocrysts are 1 to 3 mm in length. Clinopyroxene

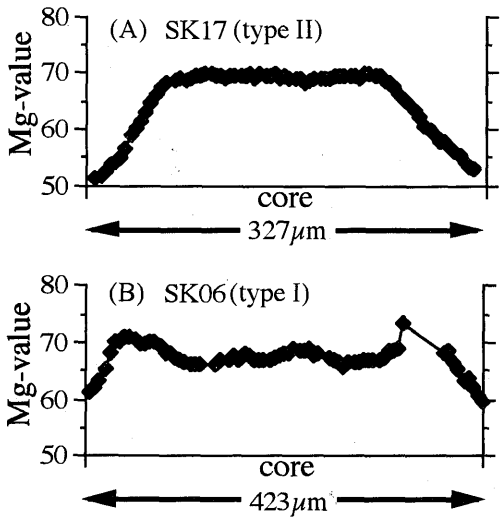

Fig. 5. Representative step scanning profiles across-orthopyroxene phenocryst from the SK andesite, showing variation in Mg values.

phenocrysts are found in samples with FeO*/MgO ratios more than 1.6. They are found as stubby prismatic grains less than 1 mm long, being often in contact with plagioclase phenocrysts and sometimes enclosed by plagioclase. Orthopyroxene phenocrysts in a differentiated basaltic andesite, CK 30 (FeO*/MgO =2.12 and 52.25 SiO_2%), occur as isolated, prismatic euhedral grains. Fe-Ti oxides (less than 0.5 mm across) are titanomagnetite. The groundmass is intergranular or intersertal in texture, and consists of plagioclase, clinopyroxene, Fe-Ti oxides, and glass.

The phenocryst assemblage and occurrence of phenocryst minerals suggest that the crystallization sequence is from olivine, through plagioclase and clinopyroxene, to orthopyroxene.

The cores for 4-25 olivine phenocryst grains in ten basalt samples show compositional ranges of Fo=80 ~87 for CK 15, CK 06, CK 12, CK 56 and CK 48, of Fo=74 ~84 for CK 60, and of Fo=64~79 for CK 04, CK 13, CK 38 and CK 31. Olivine phenocryst cores tend to gradually decrease in Fo with FeO*/MgO ratios of the rocks (from less than 1.3 to more than 1.5). They are usually normally zoned.

Clinopyroxene phenocrysts in four specimens examined have the core with the Mg-values of 68~82 for CK 13, CK 38, CK 30 and CK 31. Orthopyroxene phenocrysts in CK 30 range in Mg-value from 68 to 76, indicating partial equilibrium with the coexisting clinopyroxene with the core of 74 to 76 as Mg-value. Both clino- and ortho-pyroxene are usually normally zoned.

Geochemistry and Sr- and Nd- isotopic compositions of the late Miocene (7-9 Ma) volcanic rocks

1. Major and trace element compositions

Major and trace element analyses of ninety-eight

Table 2. Selected whole rock chemical compositions of volcanic rocks from the study area.

Sample No.	TM01	TM02	TM08	TM12	WK01	WK-02	WK03	WK04	WK05	WK06	WK07	WK08	WK09	WK10	SK02	SK03	SK04	SK06	SK07	SK08	SK09	SK10
SiO2 (%)	50.18	50.68	51.68	52.67	72.52	74.57	74.75	74.93	76.07	76.77	77.03	77.20	79.25	80.28	56.33	56.67	56.77	59.50	60.18	60.55	60.80	62.05
TiO2	1.37	1.27	1.31	1.21	0.20	0.07	0.19	0.18	0.18	0.11	0.20	0.07	0.18	0.14	0.81	0.70	0.72	0.90	0.91	0.92	0.58	1.03
Al2O3	16.90	16.71	17.12	17.11	13.31	13.83	13.19	13.37	11.19	12.12	11.66	12.48	10.84	10.48	16.16	16.01	15.98	16.50	16.14	16.21	16.83	15.48
FeO*	9.52	8.81	9.09	8.54	2.63	1.28	1.36	1.10	1.70	0.70	0.92	1.05	0.72	0.33	6.23	6.47	5.87	6.72	6.84	6.24	4.56	6.36
MnO	0.15	0.14	0.16	0.15	0.04	0.02	0.04	0.02	0.05	0.02	0.02	0.02	0.03	0.02	0.14	0.10	0.10	0.13	0.10	0.07	0.05	0.15
MgO	6.71	6.81	6.14	5.96	0.23	0.24	0.16	0.15	0.14	0.19	0.18	0.21	0.15	0.15	4.78	4.62	4.82	2.90	2.74	2.55	2.43	1.43
CaO	9.63	9.47	9.32	9.11	1.27	0.81	0.73	0.73	1.09	1.16	1.47	0.77	1.13	1.33	7.28	7.43	6.81	6.15	5.22	5.81	5.05	4.61
Na2O	2.88	3.08	3.03	3.13	5.11	3.33	5.27	5.44	4.13	3.56	3.03	3.04	3.70	3.13	2.93	2.73	3.04	4.11	3.62	3.99	3.97	3.87
K2O	0.40	0.67	0.58	0.89	2.73	4.38	3.08	2.93	2.07	3.15	2.81	3.97	2.20	2.71	1.99	1.50	1.76	1.47	1.59	1.46	2.23	2.34
P2O5	0.33	0.33	0.35	0.33	0.02	0.01	0.01	0.01	0.01	0.01	0.02	0.01	0.01	0.02	0.16	0.13	0.14	0.20	0.20	0.19	0.13	0.31
H2O (+,-)	1.23	1.41	1.67	0.53	0.99	1.72	0.45	0.25	1.83	1.11	1.98	1.20	1.52	1.03	2.58	2.80	3.00	1.18	1.78	1.07	2.13	2.58
Total	99.29	99.39	100.46	99.62	99.05	100.27	99.22	99.11	98.48	98.89	99.31	100.03	99.73	99.62	99.38	99.16	99.02	99.76	99.31	99.06	98.77	100.21
FeO*/MgO	1.42	1.29	1.48	1.43	11.29	5.25	8.76	7.56	11.99	3.67	5.11	5.09	4.90	2.20	1.30	1.40	1.22	2.32	2.49	2.45	1.87	4.45
Cr (ppm)	324	290	326	370	106	60	64	56	197	331	65	208	94	112	490	540	482	107	225	212	234	68
Nb	7.9	6.7	7.2	7.4	13.8	6.6	14.0	11.9	11.6	3.7	3.8	4.3	10.9	3.8	6.4	5.9	4.1	7.5	6	7	4.9	8
Ni	100	103	109	97	49	17	20	38	65	52	38	32	26	23	126	139	142	42	67	66	38	44
Rb	8	18	18	18	64	148	89	69	49	87	89	131	47	85	41	33	42	38	50	41	69	47
Sr	390	386	386	364	121	41	86	86	108	56	70	42	102	66	319	286	303	287	240	261	379	292
V	182	178	189	169	3	21	3	6	2	16	21	22	5	15	149	131	146	122	103	110	83	52
Y	28	27	28	34	58	40	63	41	57	21	29	37	55	31	19	20	17	35	35	36	17	43
Zr	135	135	147	156	409	96	385	390	323	113	125	78	301	113	125	117	108	175	198	198	130	180
Ba	179	190	172	171	606	876	603	602	459	560	561	824	415	519	304	267	315	310	323	328	420	365

Sample No.	SK11	SK12	SK13	SK15	SK17	SK18	SK19	CK04	CK06	CK12	CK13	CK15	CK17	CK23	CK30	CK31	CK38	CK48	CK56	CK59	CK60	CK63
SiO2 (%)	62.28	62.29	62.55	63.25	63.38	63.64	63.74	49.31	49.41	49.87	49.90	49.92	49.97	50.61	51.86	51.88	52.14	53.02	53.51	53.96	54.38	56.17
TiO2	1.06	1.04	1.24	1.10	0.94	1.07	0.89	1.63	1.27	1.23	1.53	1.30	1.33	1.33	1.44	1.69	1.41	1.11	1.12	1.18	1.13	1.01
Al2O3	15.65	15.19	15.22	15.39	14.85	15.75	14.60	16.73	16.38	17.60	17.24	16.43	17.25	17.01	17.08	16.96	17.22	16.16	16.15	15.94	15.73	16.91
FeO*	6.65	7.00	5.13	6.82	6.38	6.44	6.69	10.46	8.86	8.24	10.92	9.37	9.07	9.04	10.62	12.22	10.32	8.54	8.40	8.53	8.42	7.64
MnO	0.09	0.22	0.11	0.16	0.18	0.16	0.30	0.16	0.15	0.14	0.18	0.13	0.17	0.16	0.19	0.19	0.19	0.18	0.16	0.14	0.14	0.14
MgO	1.64	1.34	1.69	1.67	1.28	1.54	0.68	7.08	7.87	7.05	6.54	8.58	6.81	6.58	5.00	4.70	5.25	6.81	6.78	6.67	6.35	4.88
CaO	4.30	4.01	4.27	4.26	3.59	4.24	3.25	9.70	9.02	10.33	10.26	8.90	9.63	9.64	9.14	8.84	9.30	8.60	8.40	7.99	7.98	8.52
Na2O	4.44	4.70	4.22	4.68	4.85	4.68	4.74	2.95	2.66	2.91	2.71	2.79	3.00	2.98	3.08	3.38	3.00	2.67	2.77	2.91	3.06	3.12
K2O	1.60	1.67	2.13	1.67	1.73	1.64	1.77	0.41	0.75	0.43	0.33	0.83	0.38	0.41	0.61	0.48	0.60	0.77	0.91	1.22	1.18	1.03
P2O5	0.28	0.30	0.36	0.32	0.26	0.31	0.26	0.31	0.28	0.21	0.27	0.32	0.24	0.25	0.23	0.24	0.23	0.21	0.20	0.22	0.20	0.12
H2O (+,-)	1.49	1.53	2.86	0.94	2.47	0.87	3.26	1.04	2.03	1.34	0.54	1.19	1.13	1.24	0.14	0.14	0.11	1.17	0.53	0.53	0.49	0.37
Total	99.48	99.29	99.77	100.27	99.91	100.33	100.17	99.77	98.68	99.35	100.42	99.75	98.98	99.25	99.39	100.72	99.76	99.23	98.93	99.31	99.05	99.91
FeO*/MgO	4.05	5.24	3.04	4.09	5.00	4.19	9.90	1.48	1.13	1.17	1.67	1.09	1.33	1.37	2.12	2.60	1.97	1.25	1.24	1.28	1.33	1.56
Cr (ppm)	150	166	112	102	64	103	208	211	380	303	231	502	169	140	230	126	176	502	425	462	459	411
Nb	9.2	10.0	12.2	8	9.2	9.7	7.3	6.3	7.4	4.4	6	7.5	5.5	6	5.2	6.1	5.2	5.6	7.1	6.3	6.8	6
Ni	52	40	26	44	37	42	56	87	145	90	63	153	46	33	65	47	38	144	135	150	123	86
Rb	39	39	43	38	42	39	44	6	15	10	3	20	5	7	10	9	10	27	26	26	28	25
Sr	279	271	266	280	259	281	246	355	395	354	366	383	361	369	338	334	347	311	298	309	306	298
V	59	20	54	14	<1	13	<1	231	201	218	271	210	190	184	307	387	289	188	181	220	218	201
Y	45	44	49	45	49	44	44	31	29	29	33	30	29	31	29	31	32	31	31	31	33	31
Zr	179	190	319	186	194	187	200	126	126	109	122	123	137	143	110	117	111	130	137	125	128	112
Ba	320	360	415	368	362	370	398	140	213	135	140	179	145	149	148	153	146	191	200	251	259	254

TM 01～TM 12 ; TM basalt, WK 01～WK 10 ; WK rhyolite (02, 06, 07, 08, 10 : type I, 01, 03, 04, 05, 09 : type II), SK 02～SK 19, SK andesite (02～09 : type I, 10～19 : type II), CK 04～CK 63 ; CK basalt (04～38 : type II, 48～63 : type I). $FeO^* = FeO + 0.9 \cdot Fe_2O_3$.

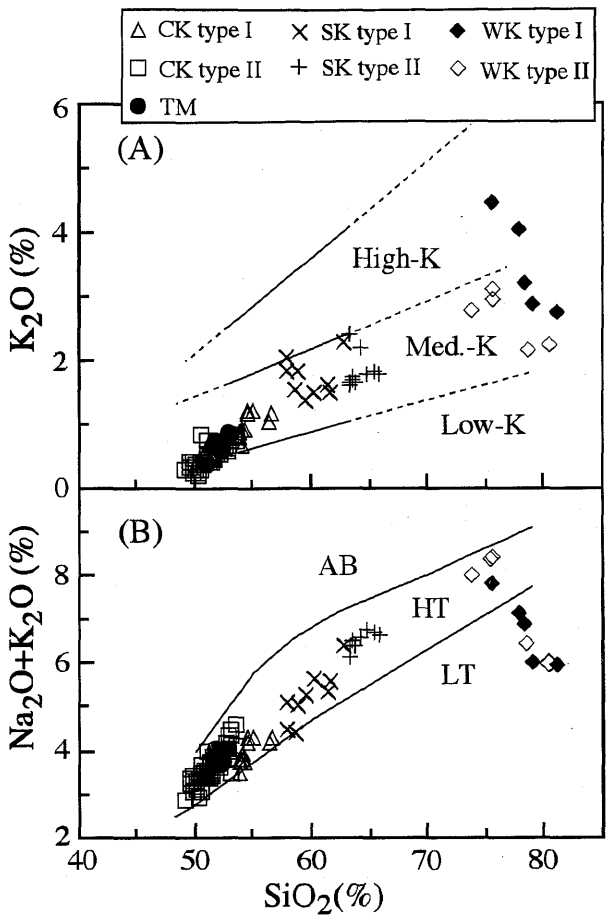

Fig. 6. SiO_2 vs. K_2O and Na_2O+K_2O variation diagrams for the 7–9 Ma volcanic rocks from the study area. The fields of low-, med.- and high-K andesites in SiO_2-K_2O diagram are from Gill (1981) and the fields of LT (low-alkali tholeiite), HT (high-alkali tholeiite) and AB (alkai basalt) in SiO_2-(Na_2O+K_2O) diagram from Kuno (1968).

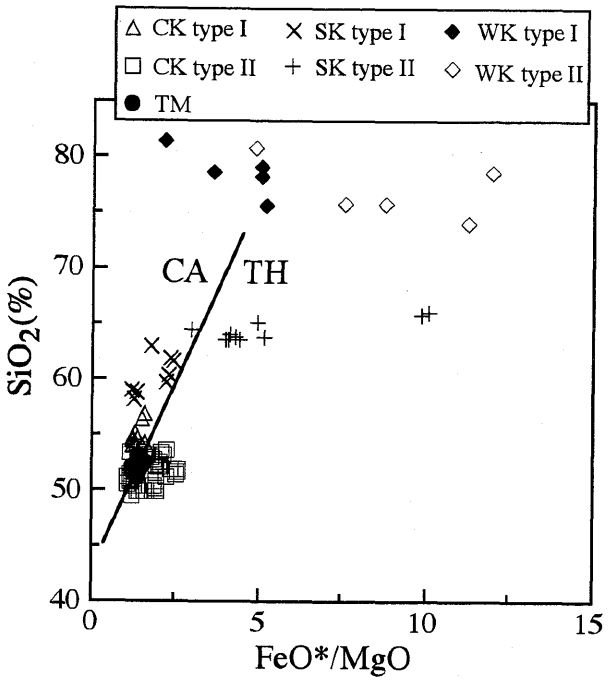

Fig. 7. FeO*/MgO vs. SiO_2 diagram for the 7–9 Ma volcanic rocks from the study area. Line shows the boundary between the fields of calc-alkaline series (CA) and tholeiitic series (TH) (after Miyashiro, 1974).

samples from the late Miocene volcanic rocks have been determined by X-ray fluorescence spectrometry at Niigata University, using analytical methods described by Tamura et al. (1989). Analyses of forty-four selected samples are listed in Table 2. In the following discussion, major element compositions are treated on an anhydrous basis, and all analyses have been plotted in Figs. 6, 7, 8 and 9.

The SiO_2 contents of basalt and andesite vary continuously from 49% to 66%, whereas there is a compositional gap of about 8% SiO_2 between the SK andesite and WK rhyolite (Fig. 6). Most rocks from the TM basalt, CK basalt and SK andesite lie within the medium-K andesite field and on its extension of Gill (1981) (Fig. 6-A), and also in the high-alkali tholeiite field of Kuno (1968) (Fig. 6-B). The WK rhyolite shows a wide variation in K_2O and Na_2O+K_2O contents, compared to basaltic and andesitic rocks, and is plotted in the medium-K and high-K andesite fields and their extensions (Fig. 6-A), and also in the low-alkali tholeiite and high-alkali tholeiite fields (Fig. 6-B).

The CK basalt, SK andesite and WK rhyolite can be divided into two groups in FeO*/MgO-SiO_2 diagram (Fig. 7) ; type I volcanic group (CK type I basalt, SK type I andesite and WK type I rhyolite) falls in the calc-alkaline (CA) field of Miyashiro (1974), where SiO_2 content increases abruptly from basalt through andesite to rhyolite despite of moderate increase in FeO*/MgO ratios, whereas type II volcanic group (CK type II basalt, SK type II andesite and WK type II rhyolite) falls in the tholeiitic (TH) field, where FeO*/MgO ratios increase from basalt through andesite to rhyolite. Since andesites with extremely high FeO*/MgO ratios (about 10) among the SK type II andesite are similar to "icelandites" of Carmichael (1964), they are termed here as icelandite-like andesite. As shown in Figs. 8 and 9, two types of volcanic group have different major and trace element abundances.

Type I of the CK basalt is relatively enriched in SiO_2, MgO, Ni and Cr compared with type II. The basalts forming lava flows in the Kakurezawa area and the northeastern part of the study area correspond to type I, whereas voluminous lava flows in the Chiyoda area correspond to type II. Type I of the SK andesite has lower SiO_2, MnO, P_2O_5, Na_2O, TiO_2, Sr, Zr, Y, Nb and V abundances than type II. Each andesite type constitutes lava flows which are separately distributed in the study area. The WK rhyolite shows a wide range for high field strength elements (HFS elements), such

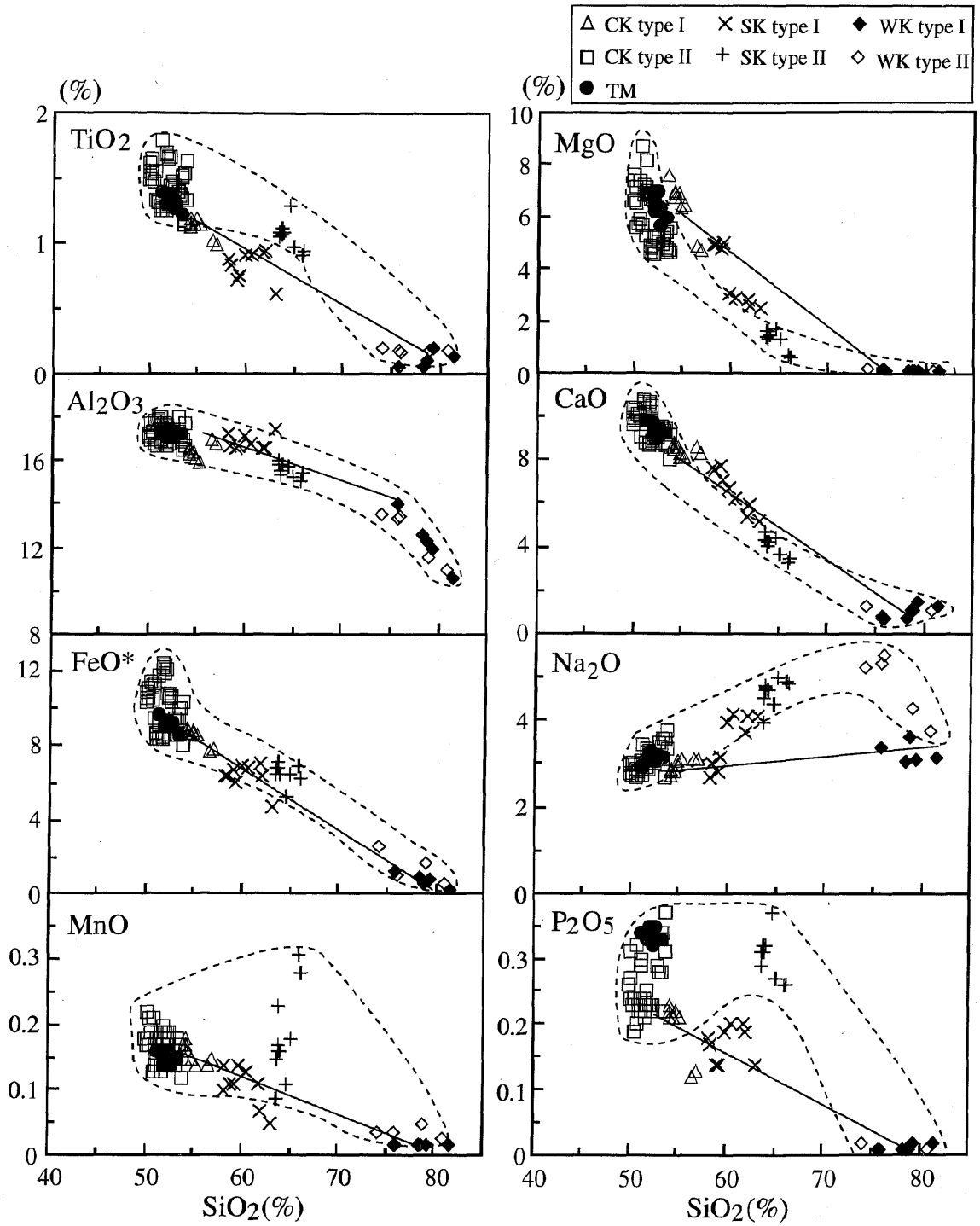

Fig. 8. SiO_2 vs. major element variation diagrams for the 7–9 Ma volcanic rocks from the study area. Solid line shows possible mixing lines between the CK type I basalt and WK type I rhyolite. Field enclosed by broken line shows the general trend of type II volcanic group.

as Zr, Nb and Y. Type I of the WK rhyolite, containing plagioclase, quartz and biotite phenocrysts, is lower in abundance of HFS elements compared with type II containnig only plagioclase phenocrysts. In general, type I has higher abundance of LIL elements, such as Rb, Ba and K_2O. Each type of the WK rhyolite also constitutes different lava flows or lava domes.

These two volcanic groups show different variation trends in Figs. 8 and 9. Major element data of type I volcanic group plot around a single line with increasing SiO_2 (Fig. 8). In contrast, the analyses of major elements of the SK type II andesite do not plot on the trends traced by type I volcanic group.

The differences between types I and II are also recognized in SiO_2-trace element variation diagrams (Fig. 9). On SiO_2-Sr, Rb, Ba, Zr, Nb, Y and V diagrams,

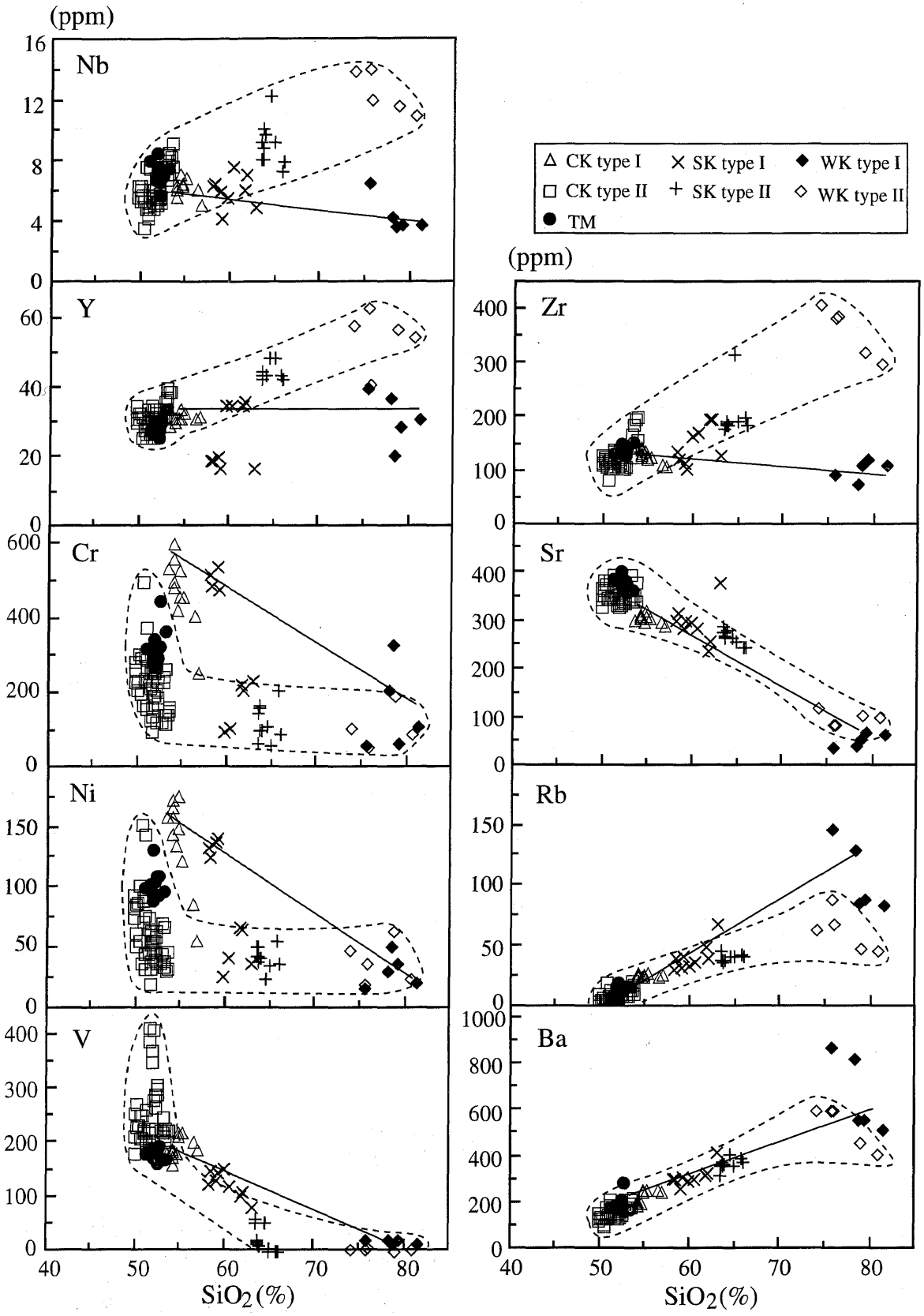

Fig. 9. SiO_2 vs. trace element variation diagrams for 7–9 Ma volcanic rocks from the study area. Solid line and field enclosed by broken line are the same as in Fig. 8.

Table 3. Sr and Nd isotopic data for the late Miocene volcanic rocks from the study area.

Name of unit	Sample number	Rock type	$^{87}Rb/^{86}Sr$	$^{87}Sr/^{86}Sr$	SrI	Sm (ppm)	Nd (ppm)	$^{147}Sm/^{144}Nd$	$^{143}Nd/^{144}Nd$	NdI	Age (Ma)
CK	CK13	Ba(II)	0.024	0.703372±17	0.703369±17	5	18	0.1679	0.512950±15	0.512933±15	7.3
basalts	CK15	Ba(II)	0.151	0.703289±14	0.703273±14	5	19	0.1591	0.512969±29	0.512953±29	7.3
	CK60	An(I)	0.265	0.703298±14	0.703270±14	4	17	0.1423	0.512948±27	0.512934±27	7.3
	CK63	An(I)	0.243	0.703375±13	0.703350±13	4	14	0.1727	0.512962±70	0.512945±70	7.3
TM	TM02	Ba	0.135	0.703355±13	0.703338±13	4	19	0.1273	0.512981±17	0.512975±17	8.7
basalts	TM08	Ba	0.135	0.703370±12	0.703353±13	5	20	0.1512	0.512985±31	0.512967±17	8.7
	TM12	Ba	0.143	0.703399±13	0.703381±13	5	20	0.1512	0.512957±41	0.512939±41	8.7
SK	SK02	An(I)	0.372	0.704142±12	0.704104±12	3	14	0.1296	0.512863±42	0.512850±42	7.2
andesites	SK04	An(I)	0.401	0.704306±11	0.704265±12	2.2	7.8	0.1705	0.512823±14	0.512815±14	7.2
	SK08	An(I)	0.454	0.703568±13	0.703522±12	3.1	10	0.1874	0.512921±13	0.512912±13	7.2
	SK09	An(I)	0.527	0.704188±14	0.704135±12	3.6	13.5	0.1612	0.512810±12	0.512804±13	7.2
	SK10	An(II)	0.466	0.703746±16	0.703699±12	3	12	0.1512	0.512947±30	0.512940±30	7.2
	SK11	An(II)	0.404	0.703798±14	0.703757±14	2.7	8	0.2041	0.512884±14	0.512874±14	7.2
	SK12	An(II)	0.416	0.703746±14	0.703703±14	2.8	8.8	0.1924	0.512916±12	0.512907±12	7.2
	SK13	An(II)	0.468	0.703523±14	0.703476±14	7	30	0.1411	0.512956±22	0.512942±22	7.2
	SK15	An(II)	0.393	0.703759±15	0.703719±15	6.2	20.3	0.1847	0.512884±11	0.512875±11	7.2
	SK17	An(II)	0.469	0.703722±14	0.703675±14	7	26	0.1628	0.512932±30	0.512916±30	7.2
	SK18	An(II)	0.401	0.703724±07	0.703683±07	6.4	21.1	0.1834	0.512894±13	0.512885±13	7.2
	SK19	An(II)	0.517	0.703777±14	0.703725±14	5.9	19.7	0.1811	0.512898±13	0.512889±13	7.2
WK	WK01	Rhy(II)	1.530	0.703727±14	0.703571±14	7.7	26.8	0.1733	0.512910±14	0.512902±14	7.0
rhyolites	WK02	Rhy(I)	10.443	0.706385±12	0.705347±12	3.3	10.6	0.1882	0.512781±14	0.512772±14	7.0
	WK03	Rhy(II)	2.993	0.703873±13	0.703574±13	9	37	0.1471	0.512950±40	0.512936±40	7.0
	WK04	Rhy(II)	2.321	0.703734±14	0.703503±13	6.9	24.5	0.1703	0.512922±13	0.512914±13	7.0
	WK05	Rhy(II)	1.312	0.703894±13	0.703764±13	8.3	29.5	0.1701	0.512894±10	0.512886±10	7.0
	WK06	Rhy(I)	4.494	0.705171±20	0.704723±20	3	15	0.1209	0.512801±25	0.512789±25	7.0
	WK07	Rhy(I)	3.678	0.705466±21	0.705100±21	3	10.2	0.1778	0.512789±13	0.512781±13	7.0
	WK08	Rhy(I)	9.023	0.706299±12	0.705402±12	3	9.4	0.1930	0.512792±13	0.512783±13	7.0
	WK09	Rhy(II)	1.333	0.703808±13	0.703676±13	6.9	23.9	0.1745	0.512899±10	0.512891±10	7.0
	WK10	Rhy(I)	3.725	0.705029±14	0.704659±14	3.3	11.6	0.1720	0.512798±13	0.512790±13	7.0

Ba ; basalt, An ; andesite, Rhy ; rhyolite, I ; type I, II ; type II, SrI ; initial $^{87}Sr/^{86}Sr$ ratio, NdI ; initial $^{143}Sr/^{144}Sr$ ratio.
K-Ar ages are from Yahata and Nishido (1995). Rb and Sr contents are shown in Table 2.

the data of type I volcanic group plot on or near the straight lines. Chromium and Ni rich samples of the SK type I andesite plot on a tie line between the CK type I basalt and WK type I rhyolite (Fig. 9). On the other hand, Zr, Nb and Y contents of type II volcanic group gradually increase with the increase in SiO_2. This is quite different from the variation trends of type I volcanic group in these diagrams (Fig. 9). In SiO_2-Cr and Ni diagrams, the contents of Ni and Cr of the CK type II basalt and SK type II andesite occupy to the below from the tie lines connecting the CK type I basalt with WK type I rhyolite, and decrease with increasing SiO_2. The WK type II rhyolite has higher Ni and Cr contents as same as those of the SK type II andesite.

2. Sr and Nd isotopic compositions

A. Analytical procedures

Extraction of Rb, Sr, Sm and Nd from rock powder has been described by Kagami et al. (1987). The mass spectrometric analysis follows the procedures of Kagami et al. (1987, 1989) and Miyazaki and Shuto (1998). The mass spectrometric analysis was conducted using MAT 262 mass spectrometer at Niigata University. $^{87}Sr/^{86}Sr$ and $^{143}Nd/^{144}Nd$ ratios were normalized to $^{86}Sr/^{88}Sr=0.1194$ and $^{146}Nd/^{144}Nd=0.7219$, respectively. Blank tests with the present analytical procedure yielded errors of 1.0 ng for Sr, 0.06 ng for Sm and 0.6 ng for Nd.

Sr isotopic ratios for NBS987 were measured ten times during this study, the average being 0.710251±0.000003 (2σ, N=51). Rb and Sr concentrations were determined by X-ray fluorescence. The mean $^{143}Nd/^{144}Nd$ ratio of JB-1a was 0.512782±0.000007 (2σ, N=9). During the course of this study, we also measured $^{143}Nd/^{144}Nd$ ratios of two the La Jolla and JNdi-1 standards, the latter of which is a new standard provided from the Geological Survey of Japan. The La Jolla standard gave a mean $^{143}Nd/^{144}Nd$ ratio of 0.511851±0.000006 (2σ, N=17) and JNdi-1 standard a mean $^{143}Nd/^{144}Nd$ ratio of 0.512106±0.000003 (2σ, N=44). Sm and Nd contents were determined with the mass spectrometer, using a ^{149}Sm-^{150}Nd mixed spike.

B. Results

The analytical results and SrI and NdI values are presented in Table 3.

Three specimens from the TM basalt have SrI be-

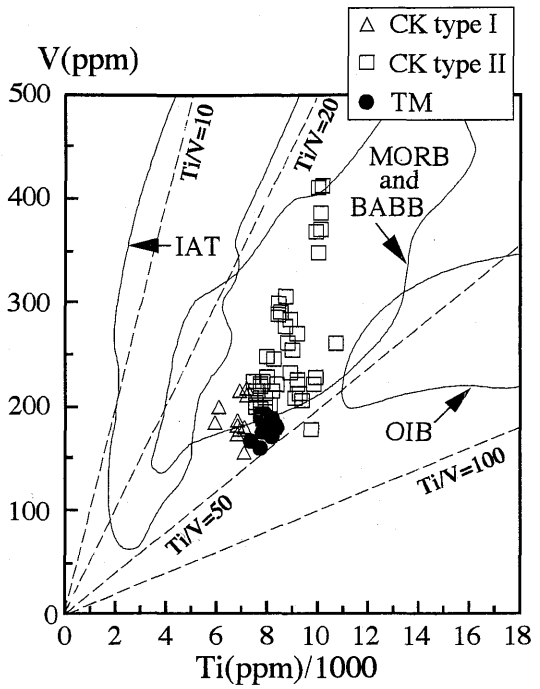

Fig. 10. V vs. Ti/1000 diagram for basaltic rocks from the study area. Fields for IAT (island arc tholeiite), MORB (mid-ocean ridge basalt) and BABB (back-arc basin basalt), and OIB (oceanic island and alkali basalt) are after Shervais (1982).

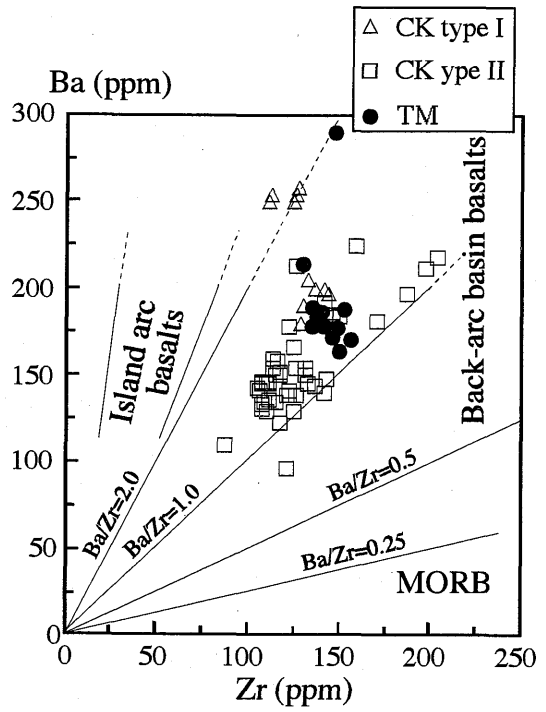

Fig. 11. Ba vs. Zr diagram for basaltic rocks from the study area. Fields for island arc basalts, back-arc basin basalts and MORB are after Saunders and Tarney (1991).

tween 0.70334 and 0.70338, and four samples from the CK basalt also have a narrow SrI range between 0.70327 and 0.70337. Both types I (CK 60 and CK 63) and type II (CK 13 and CK 15) of the CK basalt are similar in SrI to each other (Table 3). In contrast, samples from the SK andesite show a wide variation in SrI from 0.70337 to 0.70427, and the difference between types I and II of the SK andesite. The former has both higher SrI (0.70410–0.70427) and lower SrI (0.70352) than the latter ; SrI values of type II are between 0.70348–0.70376 which are slightly higher than those for the TM and CK basalts. Eleven specimens from the WK rhyolite show an wider variation in SrI than the SK andesite, and the difference between types I and II of the rhyolite. Type I rhyolite has SrI values ranging from 0.70466 to 0.70540, the highest values among the late Miocene volcanic rocks in the Engaru district, while the type II rhyolite has the SrI values between 0.70350 and 0.70376, similar to those for the SK type II andesite.

NdI values of the TM and CK basalts are between 0.51293–0.51298. These values are higher than those of the SK andesite and WK rhyolite. In contrast with SrI values, most NdI values of the SK type I andesite are lower than those of the SK type II andesite. Type I of the WK rhyolite has NdI values between 0.51277 and 0.51279, the lowest values among the measured rocks. The type II rhyolite has NdI values which are higher than those of the type I rhyolie, but similar to those of the SK type II andesite.

Generation of late Miocene andesite and rhyolite

1. Geochemical characteristics of the Tomeoka and Chiyoda-Kakurezawa basalts

As shown in Figs. 6 and 7, the CK basalt is composed of relatively primitive tholeiitic basalt (with FeO*/MgO ratios less than 1.2), evolved basalt, and basaltic andesite, all of which are characterized by intermediate K_2O and Na_2O+K_2O contents. The CK type I basalt is characterized by higher abundance of SiO_2, MgO, Ni and Cr, compared to type II basalt. The TM basalt is also tholeiitic, but shows less variability in its chemical composition (51.17–53.15% SiO_2 and 5.67–7.03% MgO) (Table 1). The TM basalt is similar in major- and trace- element contents to the CK type II basalt rather than type I basalt (Figs.8 and 9).

The Ti vs. V diagram (Fig. 10) shows that the CK and TM basalts have higher Ti contents than those of island arc tholeiite at similar V contents. These basalts are similar to MORB and BABB in terms of Ti-V relation (Fig. 10). The Zr vs. Ba diagram (Fig. 11) also shows that most rocks of the CK and TM basalts are plotted in the field of the BABB. The N-MORB-normalized incompatible element spiderdiagram for the CK and TM basalts, some island arc tholeiitic basalts from the NE Japan arc and a sample

of BABB from East Scotia Sea is shown in Fig. 12. This figure shows that HFS element abundances of the CK and TM basalts are higher than those of MORB and island arc tholeiitic basalts, but similar to those of BABB.

Thus, several trace element signature of the 7-9 Ma basalts in the study area is different from that of island arc basalts and MORB, but resembles the chemistry of BABB. Ikeda (1998) has argued, on the basis of major and trace element contents and elemental ratios, that the 7-9 Ma basaltic rocks from northeastern Hokkaido (including the present study area and its environs) have geochemical characteristics of BABB. The present data support his idea.

2. Origin of calc-alkaline WK type I rhyolite and SK type I andesite- partial melting of the crust and mixing of basaltic and rhyolitic magmas

The WK rhyolite is characterized by 1) a wide variational range in incompatible element contents (such as K_2O, Na_2O, Rb, Ba, Zr, Nb and Y) compared with the TM and CK basalts and SK andesite (Figs. 6, 7, 8 and 9), 2) differences in incompatible element contents and SrI- and NdI-values between type I and II rhyolites (Figs. 6 and 9 ; Table 3), and 3) higher SrI and lower NdI values of type I rhyolite compared the TM and CK basalts (Table 3). The latter indicates that the WK type I rhyolite cannot be formed by simple fractional crystallization of these basaltic magmas.

Crustal rocks of the Hidaka belt show a large range in SrI, from around 0.7025 to higher than 0.7060 (Shibata and Ishihara, 1979a, b ; Ikeda, 1984, 1991 ; Owada and Osanai, 1989 ; Owada et al., 1991 ; Shimura, 1992 ; Maeda and Kagami, 1994 ; Honma and Fujimaki, 1997). The SrI values of type I rhyolite are similar to those of S-type granitoids and pelitic-psammitic rocks among them. The rhyolite is peraluminous (Al/(Ca+Na+K)=>1.0), and rich in K, Rb, and Ba (Figs. 6 and 9). These features suggest either the rhyolitic magma may have assimilated granitoids and sedimentary rocks, or the source material of the magma may have contained these crustal materials. Neither xenolithic fragment nor xenocryst derived from crustal materials was observed in the WK type I rhyolite, suggesting that crustal assimilation had not an important effect on the generation of the rhyolite. Therefore, it is possible that type I rhyolite was derived by partial melting of the crust. Watanabe et al. (1995) also reported the SrI values mostly lower than 0.7040 for the middle to late Miocene rhyolites from northeastern Hokkaido, and argued that these rhyolites resulted from partial melting of the oceanic crust based on similarity in the SrI values between these rhyolites and mafic rocks of the Hidaka belt.

On the other hand, type II rhyolite is also peraluminous, but poor in K, Rb, and Ba compared with type I rhyolite (Figs. 6 and 9). The SrI values of type II rhyolite are similar to those of I-type granitoids, gabbros and MORB-type basalts of the Hidaka belt (Owada and Osanai, 1989 ; Shimura, 1992 ; Maeda and Kagami, 1994 ; Honma and Fujimaki, 1997). However, the type II rhyolite SrI values are not distinguishable from those of the SK type II andesite, and difference in SrI values between type II rhyolite and the basaltic rocks from this district is very small. Thus, it is not clear from these chemical characteristics and Sr isotopic features whether the origin of type II rhyolite is crustal melting or not.

The large differences in SrI and NdI between the SK type I andesite and basaltic rocks (TM and CK basalts) clearly indicate that type I andesite could not be derived by simple fractional crystallization of the primary basaltic magma. The SK type I andesite (such

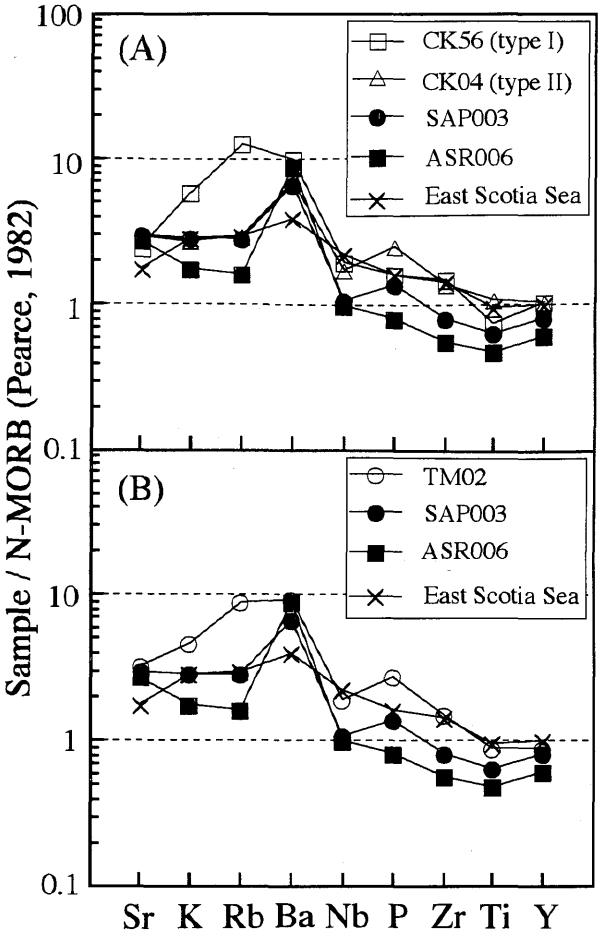

Fig. 12. Abundance pattern of incompatible elements for the CK basalt (A) and TM basalt (B) normalized to N-type MORB of Pearce (1982). Solid square and solid circle are low-K island arc tholeiites from Asari-dake and Sapporo-dake in the western region of Sapporo, respectively (Nakagawa, 1992). East Scotia Sea basalt (D23.5) is from Saunders and Tarney (1979). Basalts from the study area are selected less evolved basalts.

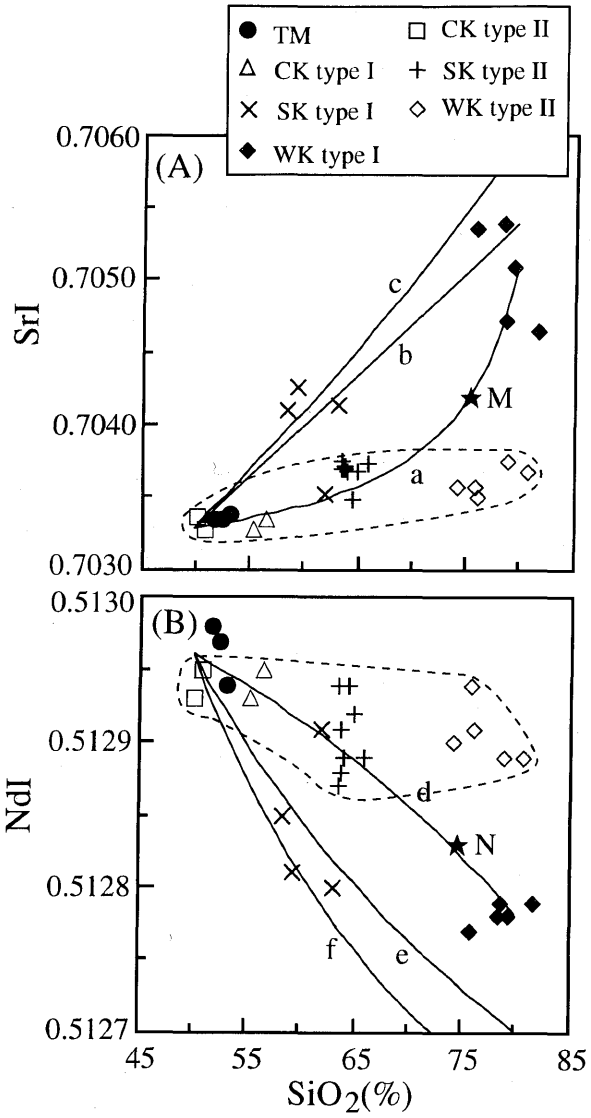

Fig. 13. SiO_2 vs. SrI and NdI diagrams for late Miocene volcanic rocks from the study area. Solid lines show calculated simple mixing curves, between the CK type I basaltic magma and rhyolitic magmas with different SrI and NdI values, and Nd and Sr contents, which were drawn using equation of Langmuir et al. (1978). End-member compositions of mixing lines in Fig. 13-A ; basaltic magma : SiO_2=50%, SrI=0.7033, Sr=300 ppm, rhyolitic magma : SiO_2=80%, SrI=0.7051, Sr=55 ppm for mixing line (a), SiO_2=80%, SrI=0.7054, Sr=300 ppm for mixing line (b), and SiO_2=80%, SrI=0.7060, Sr=250 ppm for mixing line (c). End-member compositions of mixing lines in Fig. 13-B ; basaltic magma : SiO_2=50%, NdI=0.51296, Nd=16 ppm, rhyolitic magma : SiO_2=80%, NdI=0.51278, Nd=11 ppm for mixing line (d), SiO_2=80%, NdI=0.51270, Nd=25 ppm for mixing line (e) and SiO_2=80%, NdI=0.51265, Nd=30ppm for mixing line (f). Field of type II volcanic group is enclosed by broken line. Points M and N on mixing lines (a) and (d) show the mixed magma with 75% SiO_2.

as sample SK 06) has phenocrysts showing disequilibrium relation to the coexisting liquids ; that is, 1) bimodal core compositions for orthopyroxene and clinopyroxene phenocrysts, and 2) reverse zoning of orthopyroxene and plagioclase phenocrysts. These phenomena suggest that the SK type I andesite magma resulted from mixing of magmas with different compositions.

Basaltic rocks in this district are characterized by remarkably lower SrI and higher NdI values compared with the WK type I rhyolite, and the SK type I andesite has SrI and NdI values which are roughly intermediate between those of the basalts and WK type I rhyolite. This suggests that the generation of the SK type I andesite can be ascribed to the mixing of the CK type I basaltic magma with the WK type I rhyolitic magma.

A mixing line (a) in SiO_2 vs. SrI diagram (Fig. 13-A) connects the end-member pair of the CK type I basalt (SiO_2=50%, Sr=300 ppm, SrI=0.7033) and the WK type I rhyolite (SiO_2=80%, Sr=55 ppm, SrI=0.7051). A mixing line (d) in SiO_2 vs. NdI diagram (Fig. 13-B) connects the same pair of the basalt (SiO_2=50%, Nd=16 ppm, NdI=0.51296) and the rhyolite (SiO_2=80%, Nd=11 ppm, NdI=0.51278). Although one SK type I andesite sample plots on two mixing lines (a) and (d) in Fig. 13, other three SK type I andesite samples plot away from these mixing lines.

The following possibilities for the wide deviation from the mixing lines are considered ; 1) fractional crystallization subsequent to mixing, 2) alteration or crustal assimilation after mixing, and 3) heterogeneity in Sr and Nd contents, and SrI and NdI values of the rhyolitic end-member.

The fractional crystallization of the mixed magma with about 75% SiO_2 (points M and N in Fig. 13) may result in the formation of rocks with SrI and NdI values similar to those of the above three andeistes because $^{87}Sr/^{86}Sr$ and $^{143}Nd/^{144}Nd$ ratios do not change through fractional crystallization. However, it is impossible to obtain andesitic compositions with SiO_2 content of around 60% by fractional crystallization of such mixed magma enriched in SiO_2. These andesite samples do not contain xenolithic fragments and xenocrysts, and thier phenocryst minerals and groundmass are generally fresh. These suggest that the first and second features did not give a significant effect for the wide deviation of andesite plots from the mixing lines in Fig. 13.

If the felsic end-member of the mixing line (b) in Fig. 13-A is represented by rhyolite with SiO_2 content of 80% and SrI value of 0.7054 (highest value among the WK type I rhyolite samples), its Sr content is calculated to be 300 ppm. This value is higher than the average Sr content (55 ppm) of the WK type I rhyolite. Using SrI value of 0.7060 and SiO_2 content of 80%, Sr content of the felsic end-member on the mixing line (c)

in Fig. 13-A is estimated to be 250 ppm. This Sr content is still higher than the average value of the WK type I rhyolite. The data of three andesite samples plotting away from a mixing line (d) lie near other two mixing lines (Fig. 13-B). Nd contents and NdI values of the felsic end-members containing SiO_2 content of 80% are required to be 25 ppm and 0.51270 for mixing line (e), and to be 30 ppm and 0.51265 for mixing line (f), respectively.

Consequently, more than one felsic end-member is required to explain the SrI and NdI values of the SK type I andesite in the mixing model. We can choose the following rhyolitic magmas as candidates of the felsic end-member ; 1) the WK type I rhyolite magma, and 2) rhyolite magmas with high Sr and Nd contents, and high SrI and low NdI values, compared to the WK type I rhyolite.

The mixing model is almost consistent with fact that the data of most rocks of type I volcanic group are plotted on or near mixing lines in the variation diagrams (Figs. 8 and 9). The data of some SK type I andesite samples, plotting away from the mixing lines in Figs. 8 and 9, suggest a minor degree of fractional crystallization subsequent to the mixing event. However, the data of some SK type I andesite samples plotting to the below from the mixing line in Y vs. SiO_2 daigram (Fig. 9) can not be explained by fractional crystallization. The reason for this data is ambiguous.

Thus, combined major- and trace- element and Sr- and Nd- isotopic data indicate that the mixing of basaltic magma (forming the CK type I basalt) with felsic magmas was a major process to produce the SK type I andesite. The felsic magmas are the WK type I rhyolite magma and rhyolitic magmas having higher Sr and Nd contents, and higher SrI and lower NdI values than the WK type I rhyolite magma.

3. Origin of tholeiitic WK type II rhyolite and SK type II andesite- fractional crystallization of basaltic magma

Major and trace element concentrations of type II volcanic group plot in the area which varies with increasing SiO_2, and most of the data of the SK type II andesite occupy the area apart from straight (mixing) lines linking with analyses of the CK type II basalt and WK type II rhyolite (Figs. 8 and 9). This indicates that the SK type II andesite was not derived by mixing between these basaltic and rhyolitic magmas. The concentrations of Nb, Zr and Y increase with increasing SiO_2 in type II volcanic group, and are opposite variations of type I volcanic group (Figs. 8 and 9). Moreover, Zr/Y, Zr/Nb and Y/Nb ratios of the former volcanic group either gradually increase or decrease with increasing SiO_2 (Fig. 14). The restricted values of SrI and NdI of type II volcanic group (Fig. 13) suggest the genetic relationship among the CK type II basalt, SK type II andesite and WK type II rhyolite.

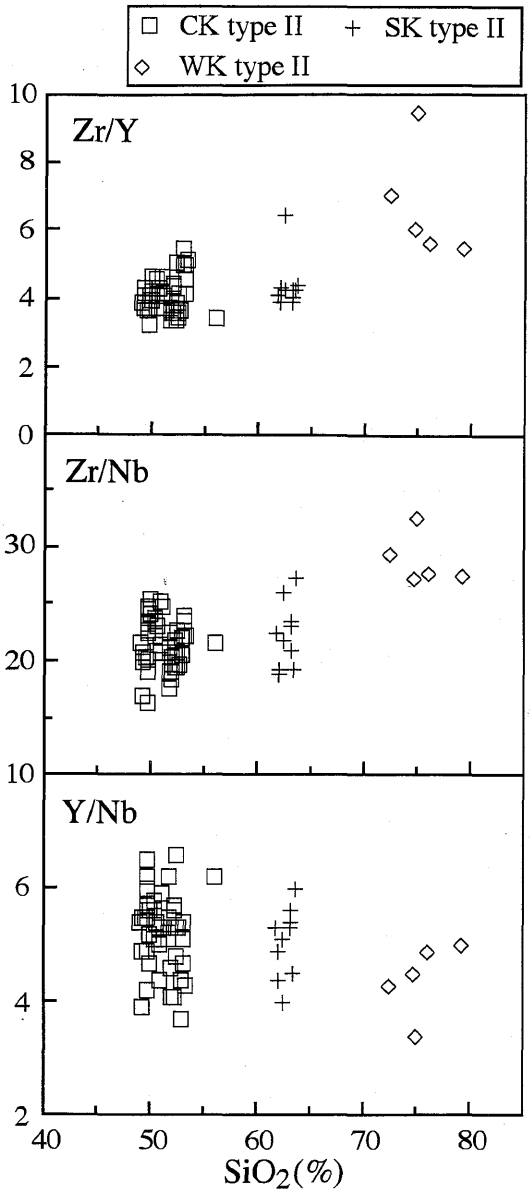

Fig. 14. SiO_2 vs. Zr/Y, Zr/Nb and Y/Nb diagrams for type II volcanic group in late Miocene volcanic rocks from the study area.

The all geochemical and Sr- and Nd- isotopic features of type II volcanic group, except MnO and P_2O_5, suggest that the SK type II andesite and WK type II rhyolite were derived mainly by fractional crystallization of basaltic magma forming the CK type II basalt. However, the causes of the enrichment in MnO in the SK type II andesite than in the CK type II basalt, and of the similar enrichment in P_2O_5 between these basalt and andesite are not clear.

Although petrographical evidences suggesting crustal assimilation are not observed in the SK type II andesite, the andesite has slightly higher SrI- and lower NdI- values than the CK type II basalt (Fig. 13).

Thus, it is probable to consider that during fractional crystallization of basaltic magma (the formation stage of the SK type II andesite), it has been somewhat affected by assimilation of crustal materials enriched in radiogenic Sr and depleted in radiogenic Nd.

Relationship between late Miocene volcanism and tectonic event

The geology in the middle to late Miocene northeastern Hokkaido is characterized by the association of non-island arc volcanic rocks, such as icelandite-like andesite and TiO_2- rich basalt and andesite, together with island arc calc-alkaline felsic rocks (Goto et al., 1995 ; Okamura et al., 1995). In addition, chemical characteristics of these volcanic rocks show no systematic regional variation such as across-arc variation in K_2O (Kokubu et al., 1994 ; Goto et al., 1995 ; Okamura et al., 1995).

Goto et al. (1995) interpreted the reason for no spatial variations in chemistry of these volcanic rocks and the appearance of non-island arc volcanism after 14 Ma, not as subduction of the Pacific plate but as the uprise of asthenospheric mantle related to spreading of the Kurile arc. Ikeda (1998) provided the same interpretation for generation of the 7–9 Ma basalts (BABB) from northeastern Hokkaido. Since spreading of the Kurile basin was considered by Kimura and Tamaki (1986) and Maeda (1990) to have been occured before 15 –16 Ma ; that is, older than the main Neogene volcanism in northern Hokkaido (Fig. 1), Okamura et al. (1995) and Watanabe (1995) considered that the volcanism was not related to spreading of the Kurile basin.

The present study has shown that the WK type I rhyolite magma could have been derived by crustal melting, and that mixing between such crust-derived rhyolitic magma and basaltic magma (originating in the upper mantle) resulted in the formation of the SK type I andesite. This implies a close relationship between basaltic magma and rhyolitic magma.

According to melting experiments of pelitic rocks under lower crustal conditions (e.g., Vielzeuf and Holloway, 1988), more than 30% of partial melts can form at temperatures higher than about 850℃. However, the thermal gradient in the lower crust beneath the most island arcs is too low to produce felsic magma by melting of the lower crust. Thus, an additional heat source is required to generate partial melting of the lower crust. The partial melting may have been caused by injection of basalt magma derived from the asthenospheric mantle. The similarity in geochemical characteristics between basaltic rocks from northeastern Hokkaido and BABB, in addition to the lack of systematic across-arc lateral variation in K_2O among the middle to late Miocene volcanic rocks in the northern Hokkaido, indicates that these basaltic magmas probably originated from a hot asthenosphere which injected into the sub-island arc mantle of northeastern Hokkaido during spreading of the Kurile basin.

The above mentioned middle to late Miocene volcanic rock association in northeastern Hokkaido is different from a typical island arc association consisting of abundant andesitic rocks and minor basaltic and dacitic rocks, such as the Quaternary volcanic zones of the Kurile and Northeast Japan arcs (e.g., Nakagawa et al., 1995 ; Yoshida and Aoki, 1984). Thus, we conclude that the middle to late Miocene volcanism in northeastern Hokkaido is not related to subduction of the Pacific plate.

Recently, based on K-Ar age data for Tertiary volcanic rocks from South Sakhalin, Takeuchi (1997) suggested that the 9–23 Ma volcanic activity in Sakhalin and Hokkaido resulted from southward migration of the Kurile during back-arc spreading of the Kurile basin and ceased at about 9 Ma. Ikeda (1998) argued that a N-S trending graben in northeastern Hokkaido (Okamura et al., 1995 ; Watanabe, 1995 ; Yahata and Nishino, 1995 ; Yahata, 1997) corresponds to the south terminate of the rift formed by the Kurile basin spreading. The results of this study may support the opinion of Ikeda (1998).

Acknowledgements

The authors wish to express their gratitude to Mr. T. Miyazaki and Dr. T. Hamamoto and Dr. M. Yuhara of Niigata Univ. for their help with Sr and Nd isotope analysis. We are also indebted to Dr. P.A. Morris of the Geological Survey of Western Australia for his revision of the English and improving the early version of manuscript. This study was supported in part by Grant-in Aid (No. 09640541) from the Japanese Ministry of Education, Science and Culture.

References

Aoki, A., Shuto, K. and Itaya, T., 1999, Stratigraphy and K-Ar ages of Tertiary volcanic rocks in the Hamamasu area, northeastern Hokkaido, Japan. *Jour. Geol. Soc. Japan*, **105**,

Carmichael, I.S.E., 1964, The petrology of Thingmuli, a Tertiary volcano in eastern Iceland. *Jour. Petrol.*, **5**, 435–460.

Gill, J.B., 1981, *Orogenic andesites and plate tectonics.* Springer-Verlag, 390 p.

Goto, Y., Nakagawa, M. and Wada, K., 1995, Tectonic setting of the Miocene volcanism in northern Hokkaido, Japan : Speculation from their K-Ar ages and major element chemistry. *Jour. Mineral. Petrol. Econ. Geol.*, **90**, 109–123.*

Honma, H. and Fujimaki, H., 1997, Rb-Sr dating and petrological characteristics of a granodiorite dike from the southern Hidaka metamorphic belt, Hokkaido, Japan. *Jour. Mineral. Petrol. Econ. Geol.*, **92**, 265–272.

Ikeda, Y., 1984, Petrological significance of granitic inclusions from Pliocene-early Pleistocene pyroclastic flow deposits in central Hokkaido, Japan. *Jour. Japan. Assoc. Mineral. Petrol. Econ. Geol.*, **79**, 60–80.

Ikeda, Y., 1991, Geochemistry and magmatic evolution of Pliocene-early Pleistocene pyroclastic flow deposits in central Hokkaido, Japan. *Jour. Geol. Soc. Japan*, **97**, 645–666.

Ikeda, Y., 1998, Geochemistry of Miocene back-arc basin basalts from northeast Hokkaido, Japan. *Jour. Geol. Soc. Japan*, **104**, 99–106.

Kagami, H., Iwata, M., Sano, S. and Honma, H., 1987, Sr and Nd isotopic compositions and Rb, Sr, Sm, and Nd concentrations of standard samples. *Tech. Rep. ISEI. Okayama Univ., Ser.B*, no. 4, 16 p.

Kagami, H., Yokose, H. and Honma, H., 1989, $^{87}Sr/^{86}Sr$ and $^{143}Nd/^{144}Nd$ ratios of GSJ rock reference samples ; JB-1 a, JA-1 and JG-1 a. *Geochem. Jour.*, **23**, 209–214.

Kimura, G. and Tamaki, K., 1986, Collision, rotation, and back-arc spreading in the region of the Okhotsk and Japan Seas. *Tectonics*, **5**, 389–401.

Kokubu, K., Okamura, S., Yahata, M., Furuyama, K. and Nagao, K., 1994, Petrological variation with time and space in the Neogene volcanic rocks from east Hokkaido. *Jour. Geol. Soc. Japan*, **100**, 658–674.*

Kuno, H., 1968, Discussion of paper by H. Aoki and M. Ito, "Rocks in the oceanic region-I. High-alumina basalts-" *Earth Science (Chikyu Kagaku)*, **22**, 195–197.**

Langmuir, C.H., Vocke, R.D., Jr., Hanson, G.N. and Hart, S.R., 1978, A general mixing equation with application to Icelandic basalts. *Earth Planet. Sci. Lett.*, **37**, 380–392.

Maeda, J., 1990, Openig of the Kurile basin deduced from the magmatic histry of Central Hokkaido, north Japan. *Tectonophys*, **174**, 235–255.

Maeda, J. and Kagami, H., 1994, Mafic igneous rocks derived from N-MORB source mantle, Hidaka magmatic zone, central Hokkaido : Sr and Nd isotopic evidence. *Jour. Geol. Soc. Japan*, **100**, 185–188.

Miyashiro, A., 1974, Volcanic rock series in island arcs and active continental margins. *Amer. Jour. Sci.*, **275**, 265–277.

Miyazaki, T. and Shuto, K., 1998, Sr and Nd isotope ratios of twelve GSJ rock reference samples. *Geochem. Jour.*, **32**, 345–350.

Nakagawa, M., 1992, Chemical zonation of volcanoes at the northern end of NE Japan arc : K-Ar ages and geochemistry of some Pliocene and Pleistocene basalts from the western region of Sapporo, southwestern Hokkaido. *Jour. Mineral. Petrol. Econ. Geol.*, **87**, 460–466.

Nakagawa, M., Goto, Y., Arai, K., Wada, K. and Itaya, T.,1993, K-Ar ages and major element chemical compositions of Late Miocene and Pliocene basalts from Takikawa district, central Hokkaido : Basaltic monogenetic volcano group at the junction of the northeastern Japan and Kurile arcs. *Jour. Mineral. Petrol. Econ. Geol.*, **88**, 390–401.*

Nakagawa, M., Maruyama, H. and Funayama, A., 1995, Distribution and spatial variation in major element chemistry of Quaternary volcanoes in Hokkaoido, Japan. *Bull. Volcanol. Soc. Japan*, **40**, 13–31.*

Okamura, S., Sugawara, M. and Kagami, H., 1995, Origin and spatial variation of Miocene volcanic rocks from north Hokkaido, Japan. *Mem. Geol. Soc. Japan*, no. 44, 165–180.*

Owada, M. and Osanai, Y., 1989, Genesis of granite in the Hidaka metamorphic belt. *Earth Monthly*, **11**, 252–257.**

Owada, M., Osanai, Y. and Kagami, H., 1991, Timing of anatexis in the Hidaka metamorphic belt, Hokkaido, Japan. *Jour. Geol. Soc. Japan*, **97**, 751–754.

Pearce, J.A., 1982, Trace element characteristics of lavas from destructive plate boundaries. *In* Thorpe, R.S., ed., *Andesites*, John Wiley and Sons, 528–548.

Saunders, A. and Tarney, J., 1979, The geochemistry of basalts from a back-arc spreading centre in the East Scotia Sea. *Geochim. Cosmochim. Acta*, **43**, 555–572.

Saunders, A. and Tarney, J., 1991, Back-arc basins. *In* Floyd, P.A., ed., *Oceanic basalts*, Blackie, 217–263.

Shervais, J.W., 1982, Ti-V plots and the petrogenesis of modern and ophiolitic lavas. *Earth Planet. Sci. Lett.*, **59**, 101–118.

Shibata, K. and Ishihara, S., 1979 a, Rb-Sr whole-rock and K-Ar mineral ages of granitic rocks in Japan. *Geochem. Jour.*, **13**, 113–119.

Shibata, K. and Ishihara, S., 1979 b, Initial $^{87}Sr/^{86}Sr$ ratios of plutonic rocks from Japan. *Contrib. Mineral. Petrol.*, **70**, 381–390.

Shibata, K., Yamaguchi, S., Ishida, M. and Nemoto, T., 1981, Geochronology of the Desmostylus —bearing formation from Utanobori, Hokkaido. *Bull. Geol. Surv. Japan*, **32**, 545–549.*

Shimura, T., 1992, Genesis and crystallization of S-type granitoid magmas. *Chikyu Monthly*, **14**, 693–699.**

Sugawara, M., Yamahana, I., Okamura, S. and Nishido, H., 1995, Miocene volcanism and primitive basalt from the Shimokawa district, north Hokkaido, Japan—constraints on Miocene tectonics from petrogenesis of primary magma—. *Mem. Geol. Soc. Japan*, no. 44, 23–37.*

Takeuchi, T., 1997, K-Ar ages of the Tertiary volcanic rocks in South Sakhalin and their tectonic significance. *Jour. Geol. Soc. Japan*, **103**, 67–97.*

Tamura, S., Kobayashi, U. and Shuto, K., 1989, Quantitative analysis of the trace elements in silicate rocks by X-ray fluorescence method. *Earth Science (Chikyu Kagaku)*, **43**, 180–185.*

Vielzeuf, D. and Holloway, J.R., 1988, Experimental determination of the fluid-absent melting relations in the pelitic system. *Contrib. Mineral. Petrol.*, **98**, 257–276.

Watanabe, Y., 1995, A tectonic model for epithermal Au mineralization in NE Hokkaido, Japan. *Resource Geol. Spec. Issue*, no. 18, 257–269.

Watanabe, Y., Kawano, Y. and Takagi, T., 1995, Rhyolites related to the Miocene epithermal gold mineralization in the Kitami region, Hokkaido, Japan. *Resource Geol. Spec. Issue*, no. 18, 237–248.

Watanabe, Y., Uchiumi, S. and Uto, K., 1991, K-Ar ages of Neogene basalts in Kitami green tuff region, northeast Hokkaido. *Jour. Geol. Soc. Japan*, **97**, 61–64.**

Watanabe, Y. and Yamaguchi, S., 1988, K-Ar ages of Miocene volcanic rocks and the tectonics in the Nayoro-Asahikawa region, northern Hokkaido. *Earth Science (Chikyu Kagaku)*, **42**, 91–99.*

Yahata, M., 1997, Neogene Monbetsu-Kamishihoro graben in the northeast Hokkaido metallogenic province, Japan. *Rept. Geol. Surv. Hokkaido*, no. 68, 43–56.*

Yahata, M. and Nishido, H., 1995, Neogene volcanism and tectonics in the Monbetsu-Engal district in the northeastern part of Central Hokkaido, Japan. *Jour. Geol. Soc. Japan*, **101**, 685–704.*

Yoshida, T. and Aoki, K., 1984, Geochemistry of major and trace elements in the Quaternary volcanic rocks. *Sci. Rep. Tohoku Univ., Ser.III*, **16**, 1–34.

* : in Japanese with English abstract

** : in Japanese

（要　旨）

Yamashita, S., Shuto, K., Kakihara, Y. and Kagami, H., 1999, Coeval volcanism due to interaction of back-arc basin basalt (BABB) magma with the island-arc crust in the late Miocene Engaru volcanic field, northeastern Hokkaido, Japan : The evidence of Sr and Nd isotopic ratios combined with major- and trace-element compositions. *Jour. Geol. Soc. Japan,* 105, 625-642.（山下智士・周藤賢治・垣原康之・加々美寛雄，1999，北部北海道，後期中新世遠軽火山活動域における背弧海盆型の玄武岩質マグマと島弧地殻の反応によって生じたマグマの同時代の活動：Sr・Nd 同位体比および主要・微量元素組成の証拠．地質雑，**105**, 625-642.）

北部北海道オホーツク海側の遠軽地域には，7-9 Ma の火山活動によって形成された大量の玄武岩（留岡（TM）玄武岩，千代田-隠沢（CK）玄武岩）と流紋岩（若松（WK）流紋岩）および少量の安山岩（栄野（SK）安山岩）を産する．玄武岩類は BABB に似た地球化学的特徴をもつ．TM 玄武岩以外の火山岩は主要・微量元素組成の特徴から 2 つのタイプに区分される．高い SrI と低い NdI をもつ WK-I 流紋岩は，地殻物質の部分溶融によって，SK-I 安山岩は，CK-I 玄武岩質マグマと WK-I 流紋岩質マグマを含む複数の流紋岩質マグマとの混合によって形成された可能性がある．一方，SK-II 安山岩と WK-II 流紋岩は，CK-II 玄武岩質マグマからの結晶分化作用によって形成された．千島海盆の拡大に伴って上昇したアセノスフェアから生じた玄武岩質マグマの添加により，地殻が部分溶融して流紋岩質マグマが生成され，さらに両マグマの混合によって安山岩が形成されたことを議論した．